UniversitatPolitècnica de Catalunya (UPC)
UniversitatAutònoma de Barcelona (UAB)
Universitat de Barcelona (UB)
Institut de CiènciesFotòniques (ICFO)

http://www.photonicsbcn.eu

Master in Photonics

MASTER THESIS WORK

Ultra-short pulse characterization, a new in-situ approach using disordered nonlinear crystals

Albert Parra Martínez

Supervised by Dr. Jose Trull (DONLL-UPC), and Dr. Crina Cojocaru (DONLL-UPC)

Presented on September 10th 2014

Registered at

Escola Tècnica Superior d'Enginyeria de Telecomunicació de Barcelona

Ultra-short pulse characterization, a new in-situ approach using disordered nonlinear crystals.

Albert Parra Martínez
"Nonlinear Dynamics, Nonlinear Optics and Lasers" Research Group (DONLL), Univ. Politècnica de Catalunya, Rambla Sant Nebridi 22, 08222 Terrassa (Barcelona, Spain)

E-mail: 1albert.parra.martinez@gmail.com

Abstract. A new single-shot assembly for ultra-short laser pulse characterization using ferroelectric crystals with inverted randomly distributed nonlinear domains is studied in detail. The second harmonic autocorrelation signal of an ultra-short pulse, generated by two noncollinear beams interaction, is recorded in the transverse direction of the pulse propagation direction. This measurement allows us to obtain the pulse duration, the chirp parameter and the initial chirped pulse duration. The experimental results are in full agreement with our theoretical predictions. The simplicity of the set-up and the theoretical method makes it very useful for in-situ pulse characterization. This novel method works for a broadband spectra, does not require angular or temperature tuning of the nonlinear crystal and allows the measurement of the pulses evolution during their propagation along the crystal.

Keywords: short pulse characterization, autocorrelation, nonlinear optics, second harmonic generation.

1 Introduction

Ultrashort pulses can be defined as those with temporal durations (*T*) less than a few hundreds of femtoseconds (10^{-15} seconds). The use of ultrashort pulses is very important in many scientific and technological applications, since they have duration shorter than atomic and molecular processes, ultra-broad spectral bandwidth and high intensity. In such applications, the proper knowledge of the pulse parameters, i.e intensity (*I*), duration (*T*), spectrum (*S*) and temporal and spectral phase, is often as important as the generation process itself.
These parameters (or properties) can be directly related to the pulse electric field, E, whose complex representation can be expressed in both, temporal or spectral domain as:

$$E(t) = E_0(t)e^{-i\omega_0 t} = \sqrt{I(t)}e^{-i\varphi(t)}e^{-i\omega_0 t} \quad \text{with} \quad E^{real}(t) = \mathrm{Re}[E(t)] \qquad (1)$$

$$\tilde{E}(\Omega) = \tilde{E}_0(\Omega)e^{-i\omega_0 t} = \sqrt{S(\Omega)}e^{-i\Psi(\Omega)}e^{-i\omega_0 t} \quad E^{real}(\Omega) = \mathrm{Re}[E(\Omega)] \qquad (2)$$

where ω_0 is the carrier frequency (or central frequency), $\phi(t)$ and $\psi(\Omega)$ are the temporal and spectral phases of the complex amplitude and $\Omega = \omega - \omega_0$. As it is well known, these two representations are linked through the Fourier-transform (FT). The temporal (spectral) phase content has influence on the pulse duration. When the spectral phase of the pulse remains constant ($\psi(\Omega)=0$) the pulse is called Fourier-transform limited (FTL) and it has the shortest temporal duration for the available bandwidth (Fig.1.1 a).
In this paper we deal mainly with Gaussian pulses, expressed through the next equations:

$$E_0(t) = Ae^{-\frac{t^2}{T^2}}e^{-i\varphi(t)} \qquad (3)$$

$$\tilde{E}_0(\Omega) = \tilde{A}e^{-\frac{\Omega^2 \cdot T^2}{4}}e^{-i\psi(\Omega)} \qquad (4)$$

where *A* is the amplitude of the pulse.

For FTL Gaussian pulses the time-bandwidth product (TBP) is $\Delta\nu\cdot\Delta\tau = 0.441$ (where $\Delta\nu=\Delta\omega/2\pi$ and $\Delta\tau$ are measured at full width half maximum (FWHM) in intensity).
If the phase is not constant a Taylor series expansion for the phase about t=0 (Ω=0) gives:

$$\varphi(t) = \varphi_0 + \varphi_1\frac{t}{1!} + \varphi_2\frac{t^2}{2!} + \varphi_3\frac{t^3}{3!} + \ldots \quad \rightarrow \quad \omega_{inst}(t) = \omega_o + \frac{d\varphi(t)}{dt} \qquad (5)$$

$$\Psi(\Omega) = \Psi_0 + \Psi_1\frac{\Omega}{1!} + \Psi_2\frac{\Omega^2}{2!} + \Psi_3\frac{\Omega^3}{3!} + \ldots \quad \rightarrow \quad T_{delay} = \frac{d\Psi(\Omega)}{d\Omega} \qquad (6)$$

A non-vanishing phase results in larger TBP and in the appearance of an instantaneous frequency $\omega(t)$ or group delay $T_{delay}(\Omega)$ in the pulse as defined in eqs. (5) and (6). In general a pulse with phase modulation will be longer than an equivalent TFL pulse with the same spectrum.
The first term in eq. (5), φ_0, is the carrier envelope phase term, which we will not consider in this work. The first order term φ_1 gives a global frequency shift, which does not affect the pulse duration. The presence of the second order term φ_2 gives an instantaneous frequency, which varies linearly with time and results in up-chirped (if $\varphi_2>0$) or down-chirped ($\varphi_2<0$) pulses (Fig.1.1 b, c). In this case the pulse is broadened and its peak intensity reduced due to the different group velocities for each frequency (Fig.1.1 a). Higher order contributions lead to pulse distortions.
In the spectral domain we find in an equivalent way the group delay, ψ_1, the group delay dispersion (GDD), ψ_2, third order dispersion (TOD), ψ_3, and so on. In the presence of TOD ($\psi_3\neq0$), the peak intensity is reduced and lateral satellites appear on the pulse (Fig.1.1 a).
When the pulse is propagating inside a dispersive media, the dependence of the index of refraction with wavelength results in the appearance of spectral phase modulation. This effect produces a phase variation of the pulse during the pulse propagation inside the material adding to ψ_2 a term $GDD_{prop}=g\cdot L$ and to ψ_3 a term $TOD_{prop}=\beta_3\cdot L$, where $g = k_\omega^{''}$ is the group velocity dispersion coefficient of the media, $\beta_3 = k_\omega^{'''}$ the third order dispersion coefficient of the material and L the propagation distance. These variations can be translated in a larger (or stronger) pulse broadening or compression as we will show in the experimental results[1]. We will neglect the higher orders that can be observed only for very short pulses.

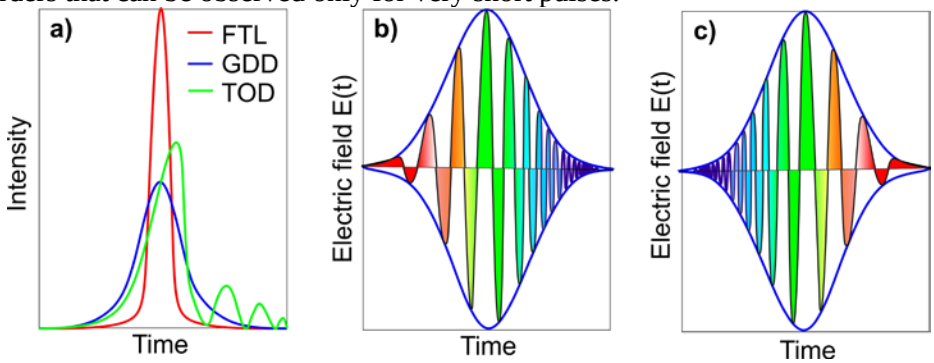

Figure 1.1: **a)** Pulse intensity profiles in FTL case (red), with initial GDD or chirp (blue) and with third order effect TOD (green).**b)** Up-chirped pulse electric field profile. **c)** Down-chirped pulse electric profile.

The temporal envelope variation of an ultrashort pulse is impossible to be detected by the response of electronic devices, as oscilloscopes or a photodiodes. This is why indirect nonlinear methods are needed for their measurement. The actually available methods can give a partial characterization (intensity and pulse duration) or provide a full reconstruction of the pulse (measurement of amplitude and phase)[2].
One of the most used methods to measure ultrashort pulses duration is the intensity autocorrelation (AC) which is based on the measurement of the AC function expressed as following:

$$A(\tau) \equiv \int_{-\infty}^{\infty} I(t)I(t-\tau)dt \qquad (7)$$

The experimental implementation of the AC method is based on the superposition of the unknown pulse E(t) with a replica of itself, retarded by a controlled delay time t = τ, within a

nonlinear crystal. The multiplication operation is provided by the use of a nonlinear effect, while the temporal integration is given by the integration due to the "slow" response of the photodiode. The intensity AC gives us partial information about the temporal duration of the pulse but in general some information concerning the pulse profile is necessary to obtain accurate results.

The nonlinear effect, called second harmonic generation (SHG), results from the combination of two photons at the same frequency (ω) (from a fundamental beam) in the nonlinear material to give one photon with twice that frequency (2ω). This effect only appears in non centro-symmetric crystals, that don't display inversion symmetry, when the phase matching (PM) condition is fulfilled (momentum conservation between the input and output photons) and the intensity is high enough to generate a polarization (P) from the crystal that depends on the second order susceptibility (χ^2).

If a complete characterization of ultrashort pulse is desired other methods giving information about both the modulus and the phase at the same time should be used. Two of these standard techniques are the Frequency-Resolved Optical Gating (FROG), based on the concept of optical gating and Direct Electric-field Reconstruction (SPIDER), based on the concept of spectral interferometry.

In this thesis we propose a new alternative single-shot method to characterize an ultrashort pulse and obtain information about its temporal duration and its chirp based on the transverse second harmonic generation by crystals with a random domain distribution of inverted nonlinear domains in a very simple configuration which allows for an in-situ pulse evaluation. In section 2, our method is explained in detail as well as some characteristics of the elements that compose it. In section 3 we show experimental results obtained with our approach using pulses with different time duration and changing its phase parameters and these results are discussed. In section 4 we explain other method called single-shot D-scan using the same kind of crystals.

2 Experimental device: structure and implementation

2.1 Second harmonic generation in disorder ferroelectric crystals

Efficient energy conversion in nonlinear parametric processes, such as SHG, requires the fulfillment of the phase matching condition, $\Delta\mathbf{k}= \mathbf{k}_{2\omega}-2\mathbf{k}_{\omega}=0$, where k_ω and $k_{2\omega}$ are the wave vectors of the fundamental and SH beam, respectively. For the SHG this means equal refractive indices for the fundamental and SH beams $n(\omega)=n(2\omega)$. When propagating in dispersive materials, the interacting waves go out of phase due to the index refraction dependence on wavelength and the energy start to flow back to de fundamental beam after a coherence length. The coherence length is defined as the material length for which the phase-mismatch between the interacting waves is π ($l_c=\pi/\Delta k$).

Traditional PM techniques are based on the use of birefringent media or quasi-phase matching (QPM) structures obtained by periodically modulating the nonlinear coefficient of the material every coherence length. In this way the phase difference is always shorter than π and produces always an energy transfer from fundamental field to the SH, achieving efficiencies close to the perfect PM. This can be understood as the momentum conservation law is fulfilled with the help of the additional grating vector **G** which describes the periodicity of the antiparallel domains, $\Delta\mathbf{k}= \mathbf{k}_{2\omega}-2\mathbf{k}_{\omega}-\mathbf{G} =0$. However, these methods can only be implemented for a particular nonlinear interaction, a specific propagation direction within the NL crystal and for a narrow set of wavelengths.

It has been demonstrated that using materials consisting of antiparallel nonlinear ferroelectric domains (with alternating sign of the nonlinear $\chi^{(2)}$ coefficient) with random sizes and spatial distribution, one can get the PM over a wide range of conditions. The linear refractive index of these materials is constant (it is not modulated). In this work we have used a nonlinear ferroelectric crystal called Strontium Barium Niobate (SBN). The disordered modulation provides a continuous set of PM gratings with various periods and in all directions of the x-y plane. The general PM condition for SHG is written as $\mathbf{k}_2= \mathbf{k}'_1+\mathbf{k}_1+\mathbf{G}$ where $\mathbf{k}'_1$, $\mathbf{k}_1$ and $\mathbf{k}_2$ are the wave vectors of the incident beams and SH waves, respectively, and G represents one of the reciprocal vectors available from the infinite set of vectors provided by a disordered ferroelectric material (Fig. 2.1 a). As a result, for any fundamental wave vector $\mathbf{k}_\omega$ and any

direction (within the plane perpendicular to the optical axis) of light propagating through the crystal there will be a matching grating vector **G** to fulfill the PM condition, providing a way to produce SHG in different directions.
In the same time, the random G vector distribution provides an achromatic PM, meaning that a broad range of frequencies can be converted with equal efficiency. The bandwidth of the SHG conversion is only limited by the transparency range of the crystal (for the SBN crystal between 370 and 2000 nm). Depending on the propagation direction of the fundamental beam, the SHG inside the SBN crystal is different. If **k** is perpendicular to the domain orientation (optical axis or z-axis) the SH light is emitted in all directions because all available vectors for PM lie in the x-y plane (planar SHG, Fig. 2.1 b). On the other hand if **k** is parallel to z-axis (perpendicular to x-y plane) the SH is emitted in the form of a radially polarized cone which angle φ depends on the phase mismatch between the incident field and the SH wave (conical SHG)[3].
In this thesis we propose the implementation of the SHG in a SBN crystal in a single-shot autocorrelation device, for the characterization of ultrashort pulses. We overlap inside the crystal the pulse to be measured and a replica of itself, forming angles of α and -α respectively with respect to the propagating axis, x, inside the crystal. With this configuration we obtain three well resolved emission patterns of SH: two cones corresponding to the independent SH signals generated by each one of the beams along their propagating directions, and a central flat emission over a plane, which corresponds to the autocorrelation between the two beams (Fig. 2.1 c). The key point of this experimental configuration is the measurement of the transverse SHG (TSHG) that can be recorded with a camera placed above the crystal, perpendicular to the propagation direction. The TSHG makes possible the observation of the evolution of the SH autocorrelation line inside the crystal and this will allow us to characterize some pulse properties as its initial duration or initial chirp and the evolution of its pulse duration (broadening or compression). Moreover, if instead of a camera we placed and spectrometer at the same position, the spectrum of the pulse during the propagation could be also obtained. These parameters can not be directly determined from the typical AC schemes, where the SH can be measured only at the output of the crystal.

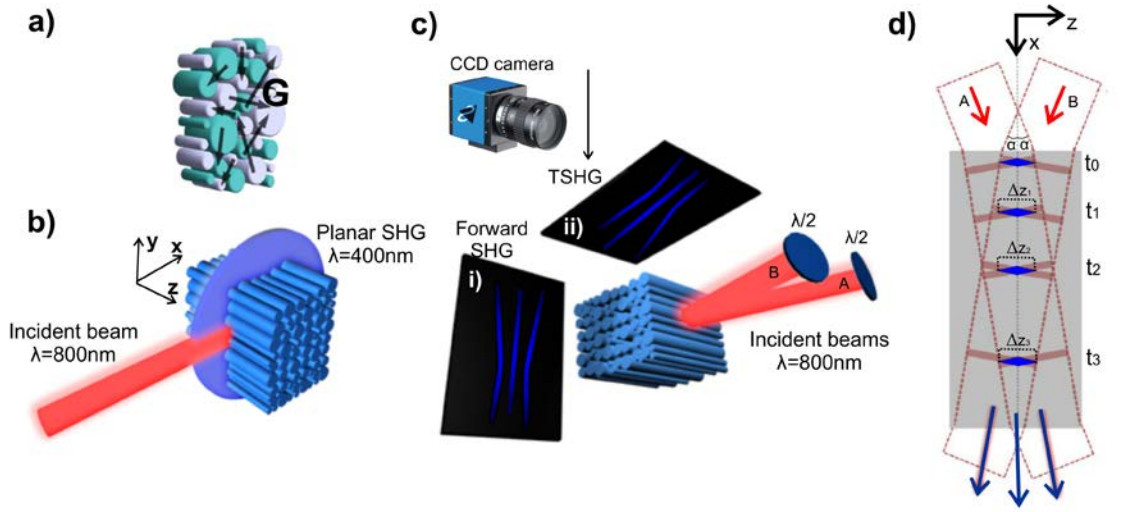

Figure 2.1: **a)** Schematic representation of the random domain distribution (x-y plane of the crystal). **b)** Schematic representation of the planar SHG from a beam propagating perpendicular to x-y plane of the crystal. **c)** Noncollinear interaction of two beams at λ=800nm, crossing along the crystal and the corresponding SHG at λ=400nm in both forward (i) and transverse (ii) directions. The central line to planar SH emission; the other ones represent the conical emission from each individual incident beams. **d)** Interaction of both incident beams inside the SBN crystal; every transverse section of this central line has all autocorrelation information with a single shot and recording this signal with a camera is possible retrieve the pulse duration (Eq. 10) measuring the width, Δz, of that central line.

Is important to comment that the initial polarization of the two incident beams is relevant in terms of efficiency and it depends on d_{eff} of each particular crystal. In SBN case, for extraordinary polarization (parallel to domain orientation) the three SH waves have the maximum intensity, for ordinary (perpendicular to domain orientation) the three lines are observed with less intensity and if one is extraordinary and the other ordinary the central

autocorrelation line is barely observed. Thus, we can control the beams polarization, using λ/2 wave plates, to improve the results.

2.2 Experimental setup

The setup used in this work is based on the method for pulse duration measurements reported in ref.[4]. Two beams propagating in the x-y plane of a SBN crystal and forming angles +α and –α with respect to the x-axis generate a SH signal in the area where the incident pulses overlap between them, as explained in the previous section. Since we deal with TSHG and not the typical forward one used in traditional pulse duration measurement techniques [5], we can measure the pulse duration at different positions within the crystal (Fig. 2.1 d). Therefore, the overlapping volume of the two pulses is moving towards the output face, resulting in a SH line. The width of the TSHG line is directly related to the pulse duration and beam size, allowing us to determine the pulse duration. This transverse SH line intensity recorded by a camera is described as the following equation[4]:

$$I_{2\omega}(z) = I_{0,2\omega} \exp\left(-\frac{2z^2 \sin^2(\alpha)}{u^2 T^2}\right) \qquad (8)$$

where u=c/n is the speed of light inside the crystal, *T* the pulse duration, α the incident angle and z the transverse direction of SH autocorrelation line.

If Δz is the pulse width at 1/e level then $I_{2\omega}(z) = I_{0,2\omega} / e$, thus:

$$\frac{2\Delta z^2 \sin^2(\alpha)}{u^2 T^2} = 1 \rightarrow T^2 = \frac{2\Delta z^2 \sin^2(\alpha)}{u^2} \qquad (9)$$

The pulse duration at FWHM is $\tau = T \cdot 2\sqrt{\ln(2)}$ and $\Delta z_{FWHM} = \Delta z \cdot 2\sqrt{\ln(2)}$. Substituting these parameters in equation 9 the following expression for pulse duration at FWHM is obtained:

$$\tau = \frac{\sqrt{2}\Delta z_{FWHM} \sin(\alpha)}{u} = \frac{\sqrt{2}\Delta z_{FWHM} \sin(\alpha_{ext})}{c} \qquad (10)$$

Monitoring the width of the TSHG line along the crystal length can provide additional information about the pulse evolution inside the crystal. In this master thesis we have extended this work to measure much shorter pulses and demonstrated that this technique allows the measurement of additional properties such as the initial chirp, which becomes increasingly important as the pulse duration is reduced since the dispersion length depends quadratically on pulse duration. Dispersion phase measurement is needed for pulses below 50 fs, since propagation along typical optical elements introduces broadening effects to them.

When the pulse has an initial chirp, $C = \varphi_2 T_0^2 / 2$, the value of *T* during propagation is given by the expression (valid up to second order in dispersion, i.e negligible TOD):

$$T^2(x) = T_0^2 \left(1 + \frac{2Sign(g)C}{L_D} x + \frac{1+C^2}{L_D^2} x^2\right) \rightarrow L_D = \frac{T_0^2}{2|g|} \qquad (11)$$

where L_D is the group velocity dispersion (GVD) length and T_0 the pulse duration (1/e in amplitude) at the entrance of the crystal. This dispersion effect during the pulse propagation results in lengthening or compression of the pulse. In normal GVD regime (g>0), group velocity decreases with increasing optical frequency, i.e. redder frequencies travel faster than bluer frequencies, thus if *C*>0 the pulse will become longer during the propagation. If *C*<0 instead, this leads to pulse compression until the different frequencies are in phase and the pulse acquires its minimum possible duration (T_{min}) corresponding to the FTL case. The distance at which the minimum pulse duration is obtained is x_{min}. In the case of anomalous GVD regime (g<0), when bluer frequencies travel faster than the redder ones, the pulse gets longer for *C*<0 and is initially compressed if *C*>0 (compression is obtained whenever C and g have different sign).

The minimum pulse duration and distance traveled inside the crystal are obtained from Eq. 11:

$$x_{\min} = \frac{C \cdot T_0^2}{2g(1+C^2)} \qquad T_{\min} = T_0 \cdot \frac{1}{\sqrt{1+C^2}} \qquad (12)$$

It is clear from the considerations above that down-chirped pulses will be compressed during propagation inside the SBN crystal (because g_{SBN}>0). The experimental determination of x_{min}

and T_{min}, should allow us to find the unknown values of initial chirp, C, and initial pulse duration using the following formulas:

$$C = \frac{2g \cdot x_{min}}{T_{min}^2} \qquad T_0 = \sqrt{T_{min}^2 + (2g \cdot x_{min})^2} \qquad (13)$$

This is the basis of the measuring method we have implemented in this master thesis work, which we will apply for the characterization of ultrashort pulses.

3 Experimental results

3.1 Measurement of pulses of the order of 200fs

The experimental work started by mounting a portable setup according to the details described above to determine the duration of fs pulses generated by a Ti:Sapphire oscillator (Mira, Coherent) operating at 800 nm, with a repetition rate of 76 MHz. Typical pulse durations are about τ_{FWHM}=200 fs, corresponding to a L_D=30 mm, so we do not expect to have significant pulse lengthening along the SBN crystal used (5x5x10mm). This is the case already reported in [4] and we used it as a first step to get used to the experimental setup.

For the measurement we adjusted the half-wavelength plates for extraordinary polarized beams and selected an external angle of intersection $2\alpha_{ext}$=10.44º. The TSHG signal, recorded using a CCD camera with 8 microns pixel size after filtering the scattered radiation at 800 nm, is shown in figure 3.1 a, b. The SH recorded includes the background of each individual beam together with the autocorrelation signal. To separate the background from the AC signal we changed the delay of one of the beams to avoid their overlapping inside the crystal. The resulting image corresponds to the background without AC (Fig. 3.1 c). After this background has been taken off from the original image, we get a clear image of the SH AC signal (Fig. 3.1 d). We have developed a code in Matlab which represents the AC trace intensity as a function of z (Fig 3.1 e) and calculate the FWHM width (Δz) for each position along the longitudinal direction, x. Using equation (10) the pulse duration is obtained. We have obtained pulse duration of 170fs at the crystal entrance. A first order polynomial curve fitting the AC trace allows getting an average value from these data, showing initial pulse duration of 170fs increasing to 180fs at the end of the crystal (Fig.3.1 f). The 10 fs change in pulse duration along 1 cm propagation distance is not accurate enough to get a good measurement of the chirp coefficient for so long pulses because the broadening is low. The precision of the measurements depends on the quality of the camera image (quantity of recorded pixels) and in the precision measurement of the incident angle α. In these measurements we have used a camera with a normal resolution. However, for this case we did not attempt to get the best image since we were just checking the setup and numerical codes developed. For the next measurements we have used a high resolution CCD camera.

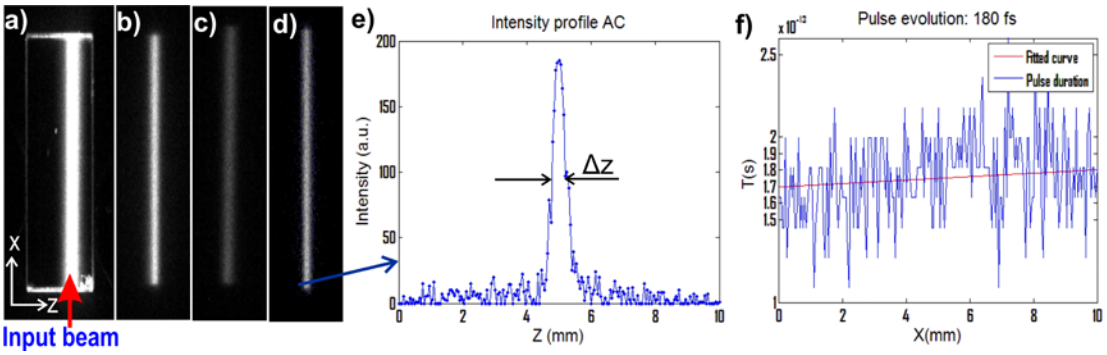

Figure 3.1: **a)** TSHG AC inside the SBN crystal illuminated with a flashlight to see the crystal. **b)** Recorded TSH signal with background. **c)** Background of the recorded signal. **d)** Clean signal without background. **e)** Intensity of the AC profile. **f)** Pulse duration evolution when propagating along the crystal (blue) and the fitted curve (red).

3.2 Measurement of 30fs pulse

Once the experimental portable setup mounted has been checked, we can use it for the characterization of much shorter pulses. In this regime the dispersion effects are much stronger since the GVD length decreases to less than 1 mm. The SBN crystal is an adequate crystal for our purpose due to its large g=466fs^2/mm at 800 nm.

The shorter pulses were generated by a Femtopower PRO 2W CEP Stabilised Laser operating at 800nm with repetition rate 1 kHz (measurements taken at CLPU Laser Facility. Salamanca). The pulse chirp could be controlled using a Dazzler (Fastlite) in order to test different input conditions into our crystal. The pulse was characterized using standard techniques such as FROG to get a comparison with our results. We used in our setup a CCD camera Spiricon SP620U with 4 microns pixel size and the imaging system was selected to provide the largest possible crystal image size into the CCD. The intersecting angle was $2\alpha_{ext}=6.8^{o}$. The laser pulses with the same initial pulse duration around 30fs at FWHM were phase modulated with a selected initial chirp using the Dazzler, before entering to our system. We selected different values in the $C<0$ regime in order to obtain compression inside the crystal. The larger the value of initial chirp, the larger should be the compression distance inside the crystal and the initial pulse duration of the incident pulse.

Figure 3.2 a) to f) shows the resulting recorded images (background corrected as explained previously) of the TSHG for different input conditions the SBN crystal (pulse propagating from bottom to top), where is clearly observed the compression and the broadening effect. Typical AC traces are shown at selected positions within the crystal in the insets. The minimum compression distance, x_{min}, and pulse duration at this point, T_{min}, are the experimental data from which we obtain the values for chirp parameter and initial pulse duration, C and T_0, using eqs. (13). T_0 cannot be retrieved from the width at the entrance of the crystal because the spatial extension of the pulses limits the overlapping region to a distance shorter than the crystal length. The pulse propagation with initial parameters C and T_o was simulated through a numerical Matlab code to compare with the experimental results. Figure 3.2 g) to l) shows the simulated traces which correspond to each experimental case. In order to check the possible effects due to TOD effects we included in the simulation the TOD term (for SBN crystal $\beta_3=360fs^3/mm$ at 800 nm)**.** We observed that for these pulses the TOD is not significant.

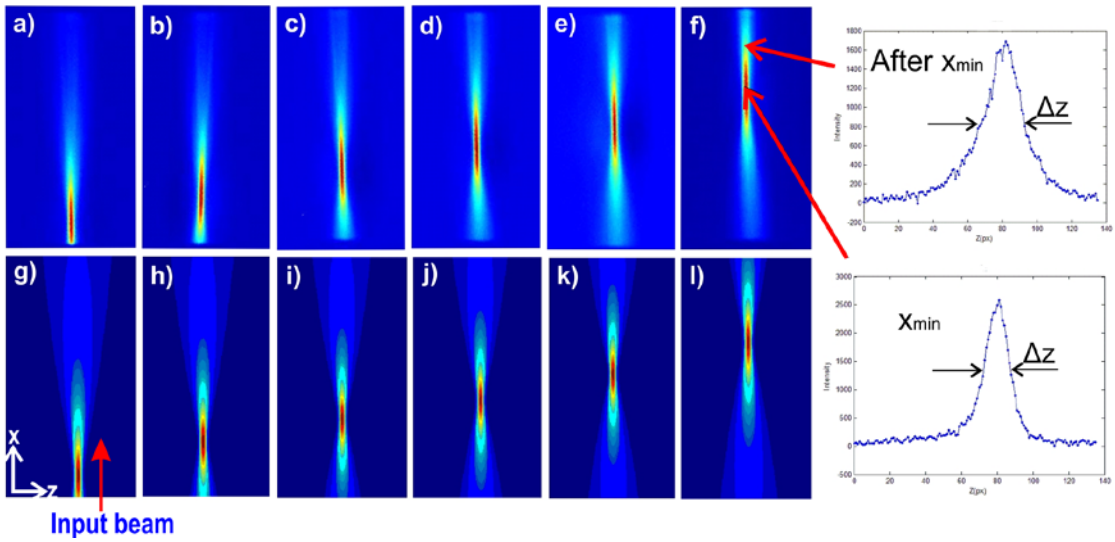

Figure 3.2: **a-f)** Experimental images of the 30fs TSHG pulses, with an increasing C from a to f. **g-l)** Theoretical images of the same pulses with same initial C (all situations correspond to initially down-chirped pulses C<0). Right side, plots of transverse intensity profiles of x_{min} and other random point, clearly the pulse duration in x_{min} is shorter.

The corresponding pulse duration (measured at FWHM) versus distance plots for the different situations, obtained from the recorded images, is shown in Figure 3.3. In this case the precision is higher because the quality of the CCD camera. The corresponding plots given by the numerical simulation are shown in figure 3.3 where a clear correspondence can be observed. A comparison of the obtained pulse durations measured with FROG technique, performed to verify our results, gives similar pulse estimation than ours.

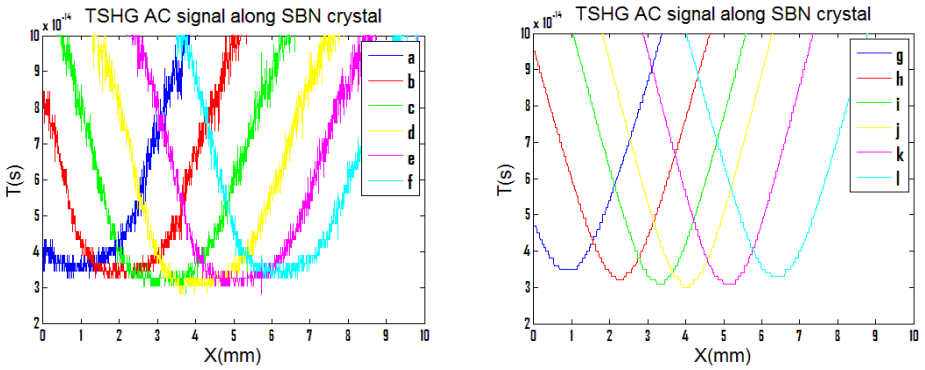

Figure 3.3: Experimental data (left) and numerical simulations (right) of the temporal pulse evolution during the propagation inside the crystal. Increasing $|C|$ the maximum compression distance x_{min} increases, but T_{min} is the same.

The results of the pulse characterization obtained in this section are resumed in Table 1. From this comparison we can see that the proposed technique works quite well for the pulse durations studied, below 50 fs, since in this regime the dispersion properties of SBN allow for a dynamic behavior of the pulse clearly measurable along the 1 cm length of our crystal. Additionally, the CCD image provides a real-time way to check the chirp content of a given pulse. The portable character of the setup makes possible to study the conditions of the pulse at the desired position within a setup thus allowing for a real time optimization of the pulse characteristics.

Table 1.Experimental obtained data and different calculated values of C, GDD and T_0. Also there is a simulation data from obtained calculations.

	Experimental data		**Calculations**			**Simulation data**	
	x_{min} (mm)	**T_{min} (fs)**	**C**	**T_0 (fs)**	**GDD(fs^2)**	**T_{min} (fs)**	**x_{min} (mm)**
A	0.88	34.41	-0.96	47.77	-411.176	35.00	0.90
B	2.26	32.44	-2.78	95.68	-1053.19	32.00	2.27
C	3.24	30.27	-4.57	141.70	-1511.25	31.00	3.30
D	4.04	30.27	-5.70	175.09	-1882.76	30.00	4.02
E	5.11	30.27	-7.21	220.46	-2384.10	31.00	5.15
F	6.40	32.44	-7.86	256.99	-2982.83	33.00	6.42

3.3 *Measurement of pulses shorter that 30fs*

In order to test the limitations of the technique we realized similar measurements with pulses of decreasing durations. To summarize we will show only the results of one of them. For these cases the SBN crystal dimensions were 5x5x5 mm, enough to see the pulse dynamics since the pulse broadening is much stronger in these cases. Surprisingly, the results show pulse durations longer than expected by a factor closely 2.

The pulses before entering in our system were carefully characterized using the d-scan technique [5] and FROG. In figure 3.4 we show a 13fs pulse measurements where our experimental results instead show pulse durations longer than 20 fs.

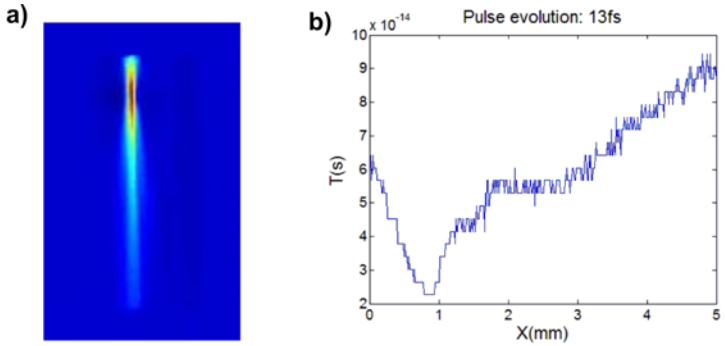

Figure 3.4: **a)** 13 fs pulse propagation along the SBN crystal recorded by a CCD camera. **b)** Is shown the pulse duration evolution during this propagation.

There are several causes that can have influence in our measurements using our technique. The pulses are too small and the coupling between them is not perfect and this can influence in

TSHG signal. With these shorter pulses there was a high instability and the background subtraction method could not work properly. Also as commented above, maybe is needed a better camera with more resolution to obtain an improved image and better method to measure the angle α with more precision. With the simulation program we study if the TOD of the SBN crystal coefficient have influence, and seems that starts to have influence for pulses with duration below than 5fs, nevertheless in the experimental could have some influence before due to small pulse distortion effects. However, these causes cannot change the pulse measurements more than few fs, not the double.

We measured the absorption for different SBN crystals (Fig. 3.5 left) that we used during all the experiments and we compared with the spectrum of both pulses obtained by d-scan technique. In this case the SBN crystal that was used is the number 3 (green and purple lines), but all have the absorption barrier almost in the same point. From λ=400nm the transmittance starts to decrease and more or less around λ=374nm we find the absorption barrier where the wavelengths below that are absorbed by the SBN crystal.

In figure 3.5 it is shown on the right the d-scan retrieval of 13fs pulse, centered at λ=780nm and is easy to see that part of the SH spectrum is below the absorption barrier. For these short pulses the central SH wavelength was λ=390 nm and their spectrum is so broad (from 350 to 440 nm), it means that not all the SH signal is transmitted in this range, and this will have an effect in our measurements especially below 374nm.

From Fourier transform relation between pulse duration and the spectrum commented in section 1, is known that shorter the pulse larger is the spectrum, because there are more planar waves with different frequency and its superposition is shorter, it means if part of the spectra is absorbed the pulse duration will be bigger, you are not measuring the pulse properly.

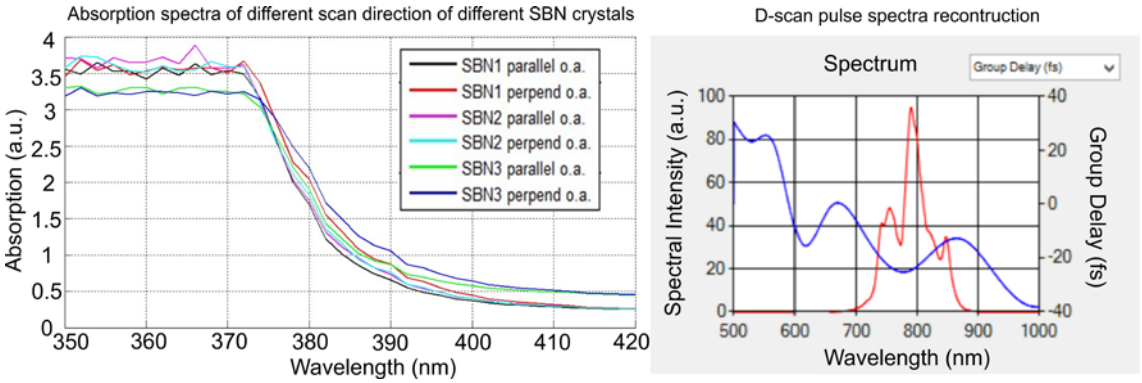

Figure 3.5: On the left is shown a plot of three different SBN crystals absorption versus the emitted wavelength. On the right is shown a spectrum trace of 13fs pulse obtained by d-scan reconstruction.

4 Single-shot d-scan

The d-scan technique is a quite recent characterization method for full-field–reconstruction which uses two crystal wedges oriented to form a plano parallel prism. Moving one of the wedges with respect to the other one can increase the total prism length, which allows introducing a selected dispersion into the pulse to be measured. The pulse SH signal, after traversing the two-wedge prism, is generated in a NL crystal and the SH spectrum is recorded in a spectrometer. The resulting d-scan trace consists on the SH spectrum as a function of the controlled dispersion introduced by the prism. An implemented algorithm reconstructs the pulse and its spectrum information [6]. This original d-scan technique is intrinsically multi-shot since the spectrum must be recorded for different thicknesses of the two-wedged prism (different dispersion values introduced in the unknown pulse to be reconstructed).

When we used this technique in our measurements for the characterization of the 13 fs pulses in section 3.3, we realised that our characterization technique could be used to achieve a single-shot implementation of the d-scan method. The role of the two-wedged prism can be replaced by the propagation inside our SBN crystal while the SH is directly performed at the same time by the same crystal, so the TSHG signal provides the SH for different propagating distances. The spectrum at each propagation distance is obtained using an imaging spectrometer. The result is a single-shot measurement of the d-scan trace.

We mounted the corresponding setup, shown schematically in Figure 4.1 left, during our stay in the CLPU laboratory, in order to check if this idea could work. The recorded single-shot d-scan trace of the first measurements of a 30fs pulse is shown in figure 4.1 right. The recorded spectral and temporal reconstruction of this pulse, using the algorithm of D-scan technique is also shown. This first trial confirms the possibilities of the method as a full-reconstruction technique. Moreover, the characteristic dispersion values of the SBN crystal, allow for pulse reconstruction of pulses in the 10-50 fs regime which is out of the measuring range of the actual d-scan technique.

Although the resolution of the d-scan trace should be improved to get acurate reconstruction results, this constitutes is a very promising result which will be further investigated and developed in the future, with a collaboration which has started in this work with the team of prof. Helder Crespo, inventor of the d-scan technique.

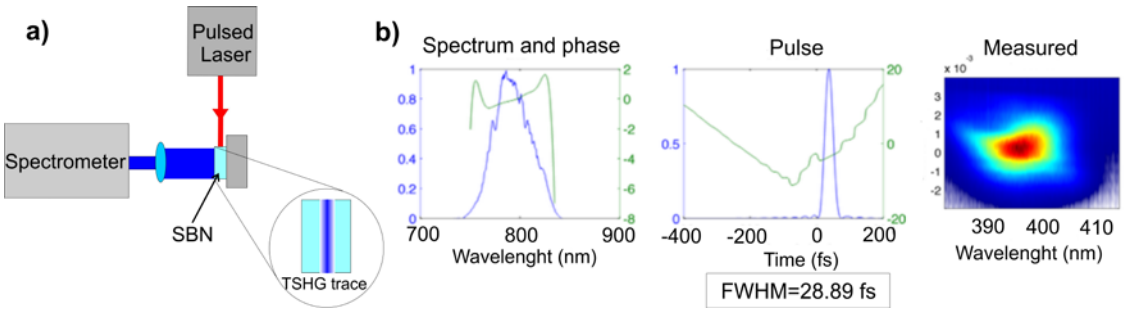

Figure 4.1: a) Is shown the single-shot d-scan setup. The pulse to be measured is incident on the SBN crystal along the x direction. The TSHG signal spectrum is measured with an imaging spectrometer. **b)** The recorded d-scan trace together with a reconstruction of the measured pulse using this technique.

5 Conclusions

Traditional autocorrelation measurement techniques present some limitations such as its narrow angular and frequency bandwidths for PM, loss of resolution due the multiple-shot character or lack of information about phase modulation of the pulses.

The single-shot set-up proposed in this work, using noncollinear TSHG propagating inside SBN crystal improves some of these limitations and extends its possibilities to chirp measurement. Recording the pulse evolution along the propagation direction within the crystal, thanks to the TSHG process provided by the disordered ferroelectric domains, is determinant for the pulse characterization process. The simplicity of the setup makes it very attractive for an in-situ approach in many different scenarios.

We have shown that this technique allows determining pulse durations and chirping coefficients for pulses down to 30 fs. For pulses shorter than 30 fs some limitations imposed by the limited spectrum range or the imaging system resolution have been observed. Our set-up can be adapted for a compact device which could provide a simple and versatile tool for experimental in-situ pulse characterization.

In addition, a single-shot d-scan technique was tested by the first time. This technique based on the properties of random NL domain crystals provides a very powerful tool for a full-field pulse reconstruction which extends considerably the capabilities of the method. However, this deserves a much deeper study in future work.

6 Acknowledgments

I'm deeply grateful to have had both the Dr. Jose Trull and Dr. Crina Cojocaru as advisors. I want also to thank my family and friends for their support these last four years.

7 References

[1] Diels J-C, Wolfgang R. Ultrashort laser pulse phenomena. Academic Press, San Diego.
[2] Walmsley I, Dorrer C. Characterization of ultrashort electromagnetic pulses. *Adv Opt Photonics* 2009;1:308.
[3] Tunyagi AR. Non-Collinear Second Harmonic Generation in Strontium Barium Niobate. 2004.
[4] Trull J et al. Characterization of femtosecond pulses via transverse second-harmonic generation in random nonlinear media. Appl Phys B 2009;95:609–15.
[5] J. Janzsky, G. Corradian,R.N. Gyuzalian, *Optics Communications* **23**, 293 1977
[6] Miranda M et al. Simultaneous compression and characterization of ultrashort laser pulses using chirped mirrors and glass wedges 2012;20:1474–6.